

Qualitative Analysis of Food-Web Model through Diffusion-Driven Instability

Chetan Swarup

Department of Basic Sciences, College of Science and Theoretical Studies, Saudi Electronic University, Riyadh-Male Campus, Riyadh, 13316, Saudi Arabia

Received June 22, 2022; Revised September 17, 2022; Accepted October 24, 2022

Cite This Paper in the Following Citation Styles

(a): [1] Chetan Swarup, "Qualitative Analysis of Food-Web Model through Diffusion-Driven Instability," *Mathematics and Statistics*, Vol. 10, No. 6, pp. 1159 - 1165, 2022. DOI: 10.13189/ms.2022.100602.

(b): Chetan Swarup (2022). *Qualitative Analysis of Food-Web Model through Diffusion-Driven Instability*. *Mathematics and Statistics*, 10(6), 1159 - 1165. DOI: 10.13189/ms.2022.100602.

Copyright©2022 by authors, all rights reserved. Authors agree that this article remains permanently open access under the terms of the Creative Commons Attribution License 4.0 International License

Abstract Many food webs exist in the ecosystem, and their survival is directly dependent on the growth rate of primary prey; it balances the entire ecosystem. The spatiotemporal dynamics of three species' food webs was proposed and analyzed in this paper, where the intermediate predator's predation term follows Holling Type IV and the top predator's predation term follows Holling Type II. To begin, we examine the system's stability using linear stability analysis. We first obtained an equilibrium solution set and then used a Jacobian method to investigate the system's stability at a biologically feasible equilibrium point. We investigate random movement in species in the presence of diffusion, establish conditions for system stability, and derive the Turing instability condition. Following that, the Turing instability condition for a spatial food web system is calculated. Finally, numerical simulations are used to validate the findings. We discovered several intriguing spatial patterns (spots, strip, and mixed patterns) that help us understand the dynamics of the real-world food web. As a result, the Turing instability analysis used in the complex food web system is especially relevant experimentally because the associated consequences can be researched and applied to a wide range of mathematical, ecological, and biological models.

Keywords Linear Stability Analysis, Turing

Instability Analysis, Food Web Model

1. Introduction

The study of the prey-predator model in an ecological system is currently the most popular topic among scholars. The food web of two species, one prey and one predator, has been the subject of traditional ecological models of interacting species. Several functional responses, such as Holling Type II, Holling Type III, Beddington-DeAngelis, and ratio-dependent type [1-4], have been studied and are still being studied. Though, it has been discovered that models based on two species can only describe a tiny number of ecosystem phenomena. Researchers have been studying three species of the food web and more for the past three decades in order to better understand the complicated dynamical behavior of species in the ecosystem. The most realistic and natural three-species food chain is one in which the middle predator is a specialist (species that can survive in the presence of preferred food). Another is that the top predator is a generalist (a species that can survive without its preferred meal), according to [5-8]. We looked at a three-species food chain in our post, with prey, middle, and apex predators.

Ali [6] investigated the system’s boundedness, existence, and stability, and we improved it by including the diffusion factor in the model. After the addition of diffusion, it is feasible to examine spatiotemporal dynamics, which will result in spatial patterns known as Turing patterns, which will increase our understanding of the real-world food web. Turing patterns were first proposed by A.M. Turing in 1952, and Levin and Jackson were the first to use them in the spatiotemporal model [9-11].

Understanding the non-homogeneous distribution of integrant species of food web over their habitat, which is fundamentally the basic block of the ecosystem, is becoming a growing and fascinating area of research in the three species food web. Segal and Jackson used the Turing instability concept, which resulted in the production of diverse patterns (spots, stripes, and mixed) [12-16].

The following is a breakdown of the paper’s structure: The detailed diffusive model is discussed in Sec. 2. In Sec. 3, local linear stability is examined. The condition of Turing instability for the system is derived in Sec. 4. Numerical simulation is used to verify the results in Sec. 5. The conclusion is derived in Sec. 6.

2. The Model

Here, we consider the food web system of three species. The population density of species is: top predator = $\rho(t)$, middle predator = $\psi(t)$ and prey = $\phi(t)$ respectively at time t . The middle predator’s predation term is based on a modified Holling type-IV functional response, whereas the top predator’s predation term is based on a Holling type- II functional response. The dynamics of food web species with diffusions is in the form of differential equations, expressed as:

$$\begin{aligned} \frac{\partial \phi}{\partial t} &= \phi(\alpha_1 - \beta_1 \phi) - \frac{b_0 \phi \psi}{s_1 + \phi} + d_1 \nabla^2 \phi = f(\phi, \psi, \rho) \\ \frac{\partial \psi}{\partial t} &= \frac{b_1 \phi \psi}{s_1 + \phi} - \gamma_1 \psi - \frac{b_2 \psi \rho}{s_2 + \psi^2} + d_2 \nabla^2 \psi = g(\phi, \psi, \rho) \\ \frac{\partial \rho}{\partial t} &= \frac{b_3 \psi \rho}{s_2 + \psi^2} - \gamma_2 \rho + d_3 \nabla^2 \rho = h(\phi, \psi, \rho) \end{aligned} \quad (1)$$

based on the aforementioned functional response, with the following initial conditions:

$$\phi(r, 0) > 0, \psi(r, 0) > 0, \rho(r, 0) > 0, \text{ for } r \in \Omega \quad (2)$$

and Neumann’s boundary condition

$$\frac{\partial \phi}{\partial \nu} = \frac{\partial \psi}{\partial \nu} = \frac{\partial \rho}{\partial \nu} = 0, \quad r \in \partial \Omega, t \geq 0 \quad (3)$$

where $\frac{\partial}{\partial \nu}$ represents the normal derivative along unit outward normal vector to $\partial \Omega$.

In model (1), α_1 and β_1 represent the growth rate and occurring competition among individuals of prey species ϕ ; s'_i ($i = 1, 2$) is the half saturation constant, γ_i ($i = 1, 2$) represents the death rate; b_0 and b_1 are the maximum values which per capital reduction rate can ϕ attain; b_2 and b_3 are the maximum values which per capital

reduction rate can ψ attain; d_1, d_2 and d_3 are the non-negative diffusion coefficients of prey, middle predator and top predator respectively.

∇^2 is the Laplacian operator in two-dimensional space.

Here, $\phi(r, t) > 0, \psi(r, t) > 0$ and $\rho(r, t) > 0$ where $r = (x, y)$ is position vector and all the parameters of model (1) are non-negative.

3. Equilibrium and Local Stability

For co-existence equilibrium point $E^* = (\phi^*, \psi^*, \rho^*)$, substituting right hand side of (1) is equal to zero without diffusion.

$$\begin{aligned} \phi(\alpha_1 - \beta_1 \phi) - \frac{b_0 \phi \psi}{s_1 + \phi} &= 0, \\ \frac{b_1 \phi \psi}{s_1 + \phi} - \gamma_1 \psi - \frac{b_2 \psi \rho}{s_2 + \psi^2} &= 0, \\ \frac{b_3 \psi \rho}{s_2 + \psi^2} - \gamma_2 \rho &= 0 \end{aligned} \quad (4)$$

From above, the following equilibrium points of system (1) are in existence:

1. $E_0 = (0, 0, 0)$, the trivial equilibrium point and always stable.
2. $E_1 = (\phi_1, 0, 0)$, the equilibrium point where only prey exists in the system.
3. $E_2 = (\phi_2, \psi_2, 0)$ is the equilibrium point when there is no top predator is present.
4. When there is no prey in the system, the existence of both the middle predator and top predator is not possible.
5. $E^* = (\phi^*, \psi^*, \rho^*)$ is the unique interior equilibrium where all three species are present.

Where $\psi^* = \frac{\gamma_2 s_2}{b_3 - \gamma_2}$, $\rho^* = \frac{(s_2 + \psi^*)}{b_2} \left(\frac{b_1 \phi^*}{s_1 + \phi^*} - \gamma_1 \right)$ and ϕ^* are the root of the following equations

$$\phi^3 - \frac{\alpha_1}{\beta_1} \phi^2 + s_1 \phi + \left[\frac{1}{\beta_1} (b_0 \psi^* - \alpha_1 s_1) \right] = 0 \quad (5)$$

Since, we are interested in the studying at the equilibrium point, where all three species are present in the food web i.e. $E^* = (\phi^*, \psi^*, \rho^*)$. Therefore, the corresponding Jacobian matrix about equilibrium points E^* is

$$J_{(\phi^*, \psi^*, \rho^*)} = \begin{bmatrix} f_\phi & f_\psi & f_\rho \\ g_\phi & g_\psi & g_\rho \\ h_\phi & h_\psi & h_\rho \end{bmatrix}$$

where

$$\begin{aligned} f_\phi &= \alpha_1 - 2\beta_1 \phi^* - \frac{b_0 \psi^*}{\phi^{*2} + s_1} + \frac{2b_0 \phi^{*2} \psi^*}{(\phi^{*2} + s_1)^2}, \\ f_\psi &= -\frac{b_0 \phi^*}{\phi^{*2} + s_1}, \quad f_\rho = 0, \\ g_\phi &= \frac{b_1 \psi^*}{\phi^{*2} + s_1} - \frac{2b_1 \phi^{*2} \psi^*}{(\phi^{*2} + s_1)^2}, \end{aligned}$$

$$g_\psi = \frac{b_1\phi^*}{\phi^{*2}+s_1} - \gamma_1 - \frac{b_2\rho^*}{s_2+\psi^*} + \frac{b_2\psi^*\rho^*}{(s_2+\psi^*)^2}, \quad g_\rho = -\frac{b_2\psi^*}{s_2+\psi^*},$$

$$h_\phi = 0, \quad h_\psi = \frac{b_3}{s_2+\psi^*} - \frac{b_3\psi^*}{(s_2+\psi^*)^2},$$

$$h_\rho = \frac{b_3\psi^*}{s_2+\psi^*} - \gamma_2$$

The condition when the uniform steady state of reaction-diffusion system is stable for ODE, but unstable in PDE with diffusion is called Turing condition. After introducing small perturbations to the homogeneous steady state $E^* = (\phi^*, \psi^*, \rho^*)$ the solution is in the form:

$$\begin{bmatrix} \phi \\ \psi \end{bmatrix} = \begin{bmatrix} \phi^* \\ \psi^* \end{bmatrix} + \varepsilon \begin{bmatrix} \bar{\phi} \\ \bar{\psi} \\ \bar{\rho} \end{bmatrix} \exp(\sigma t + ik.r) + c.c \quad (6)$$

where σ is perturbations growth rate, $0 < \varepsilon \ll 1$, $c.c.$ is complex conjugate and k is the wave number given by $k^2 = k_x^2 + k_y^2$

On substituting (6) into (1) and $\det[J^*] = 0$, the corresponding characteristic polynomial for the growth rate σ is given by:

$$J^* = \begin{bmatrix} f_\phi - d_1k^2 - \sigma & f_\psi & f_\rho \\ g_\phi & g_\psi - d_2k^2 - \sigma & g_\rho \\ h_\phi & h_\psi & h_\rho - d_3k^2 - \sigma \end{bmatrix} \quad (7)$$

$$\sigma^3 + Y_1(k^2)\sigma^2 + Y_2(k^2)\sigma + Y_3(k^2) = 0 \quad (8)$$

where

$$Y_1(k^2) = (d_1 + d_2 + d_3)k^2 - (f_\phi + g_\psi + h_\rho),$$

$$Y_2(k^2) = (d_1d_2 + d_2d_3 + d_1d_3)k^4 - [d_1(g_\psi + h_\rho) + d_2(f_\phi + h_\rho) + d_3(f_\phi + g_\psi)]k^2 + [(f_\phi + g_\psi)h_\rho - (f_\psi g_\phi - f_\phi g_\psi) - g_\rho h_\psi], \quad (9)$$

$$Y_3(k^2) = (d_1d_2d_3)k^6 - [f_\phi d_2d_3 + g_\psi d_1d_3 + h_\rho d_1d_2]k^4 + [d_1(g_\psi h_\rho - g_\rho h_\psi) + d_2 f_\phi h_\rho + d_3(f_\phi g_\psi - f_\psi g_\phi)]k^2 + [(f_\psi g_\phi - f_\phi g_\psi)h_\rho + f_\psi g_\rho h_\psi],$$

Using Routh-Hurwitz criterion, the model (1) is locally asymptotically stable at $E^* = (\phi^*, \psi^*, \rho^*)$ if;

1. $\det[J^*] < 0$,
2. $\text{tr}[J^*] < 0$,
3. $M_{11} + M_{22} + M_{33} > 0$,
4. $\text{tr}[J^*] (M_{11} + M_{22} + M_{33}) - \det[J^*] < 0$.

Contradiction of any one of the above conditions implies the existence of an eigenvalue with real part, hence Turing instability

Turing – Function

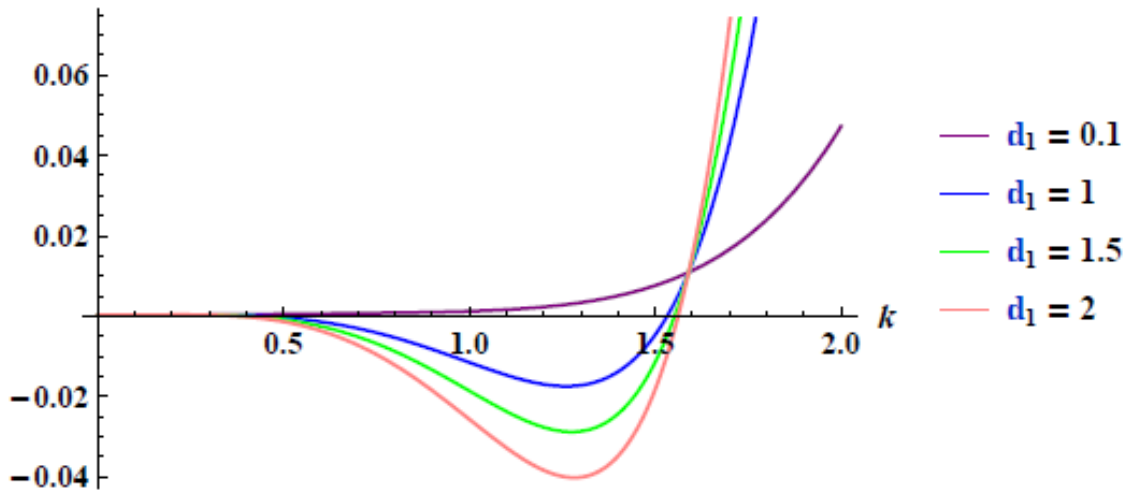


Figure 1. The region for the origination of pattern formation corresponding to Turing instability with different values of diffusion coefficient d_1 and other fixed parameters: $\alpha_1 = 0.2, \beta_1 = 0.3, b_0 = 0.1, s_1 = 1.0, b_1 = 0.3, \gamma_1 = 0.017, b_2 = 0.29, s_2 = 2.0, b_3 = 0.095, \gamma_2 = 0.025, d_2 = 0.01$ and $d_3 = 1$

4. Turing Instability

Turing instability of the diffusive model (1) occurs when the temporal steady state is locally asymptotically stable in non-diffusive system can become unstable in the corresponding diffusive system. Turing instability for (1), occurs if at least one root of Eq. (8), has a positive real part for some $k \geq 0$, while the other two eigenvalues still have a negative real part.

Therefore, diffusion driven instability occurs when $Y_3(k^2) \leq 0$ holds for at least one k . Hence condition for diffusion instability is given by

$$Y_3(k^2) = \Lambda_1(k^2)^3 + \Lambda_2(k^2)^2 + \Lambda_3(k^2) + \Lambda_4 < 0 \tag{10}$$

where

$$\Lambda_1 = d_1 d_2 d_3,$$

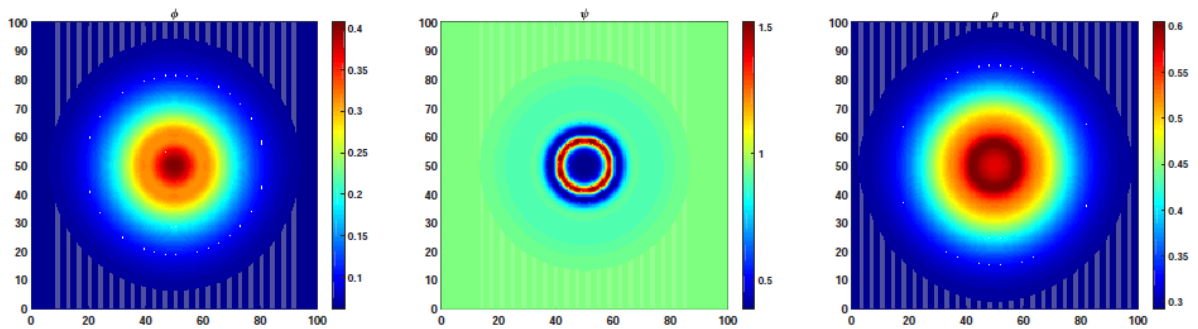
$$\Lambda_2 = -(f_\phi d_2 d_3 + g_\psi d_1 d_3 + h_\rho d_1 d_2),$$

$$\Lambda_3 = d_1(g_\psi h_\rho - g_\rho h_\psi) + d_2 f_\phi h_\rho + d_3(f_\phi g_\psi - f_\psi g_\phi),$$

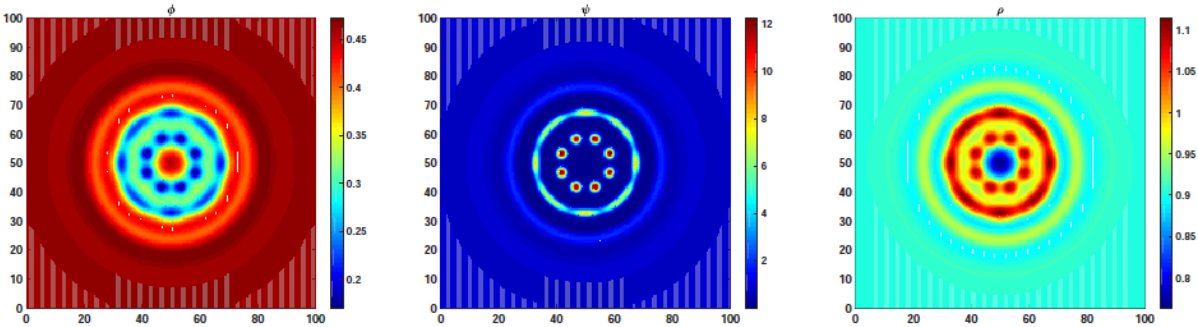
$$\Lambda_4 = (f_\psi g_\phi - f_\phi g_\psi)h_\rho + f_\psi g_\rho h_\psi.$$

The minimum value of $Y_3(k^2)$ occurs when $\frac{dY_3(k^2)}{d(k^2)} = 0$ and $\frac{d^2Y_3(k^2)}{d(k^2)^2} > 0$ at $k = k_T$ for positive value of k_T , $\Lambda_1 > 0, \Lambda_2 < 0, \Lambda_4 > 0$ and $\Lambda_2^2 > 3\Lambda_1\Lambda_3$ i.e.,

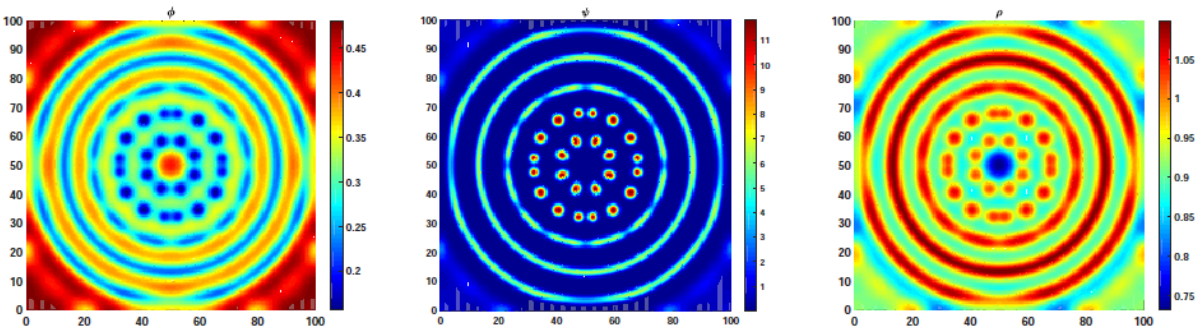
$$\begin{aligned} & (d_2(d_3f_\phi + d_1h_\rho) + d_1d_3g_\psi)^2 \\ & - 3d_1d_2d_3(d_1(g_\psi h_\rho - g_\rho h_\psi) \\ & + d_2f_\phi h_\rho + d_3(f_\phi g_\psi - f_\psi g_\phi)) \\ & > 0 \end{aligned}$$



1. At 1,000 Iterations



2. At 5,000 Iterations



3. At 10,000 Iterations

Figure 2. Snapshots of contour pictures of species ' ϕ ', ' ψ ' and ' ρ ' with $d_1 = 2$ and other parameters : $\alpha_1 = 0.2, \beta_1 = 0.3, b_0 = 0.1, s_1 = 1.0, b_1 = 0.3, \gamma_1 = 0.017, b_2 = 0.29, s_2 = 2.0, b_3 = 0.095, \gamma_2 = 0.025, d_2 = 0.01$ and $d_3 = 1$

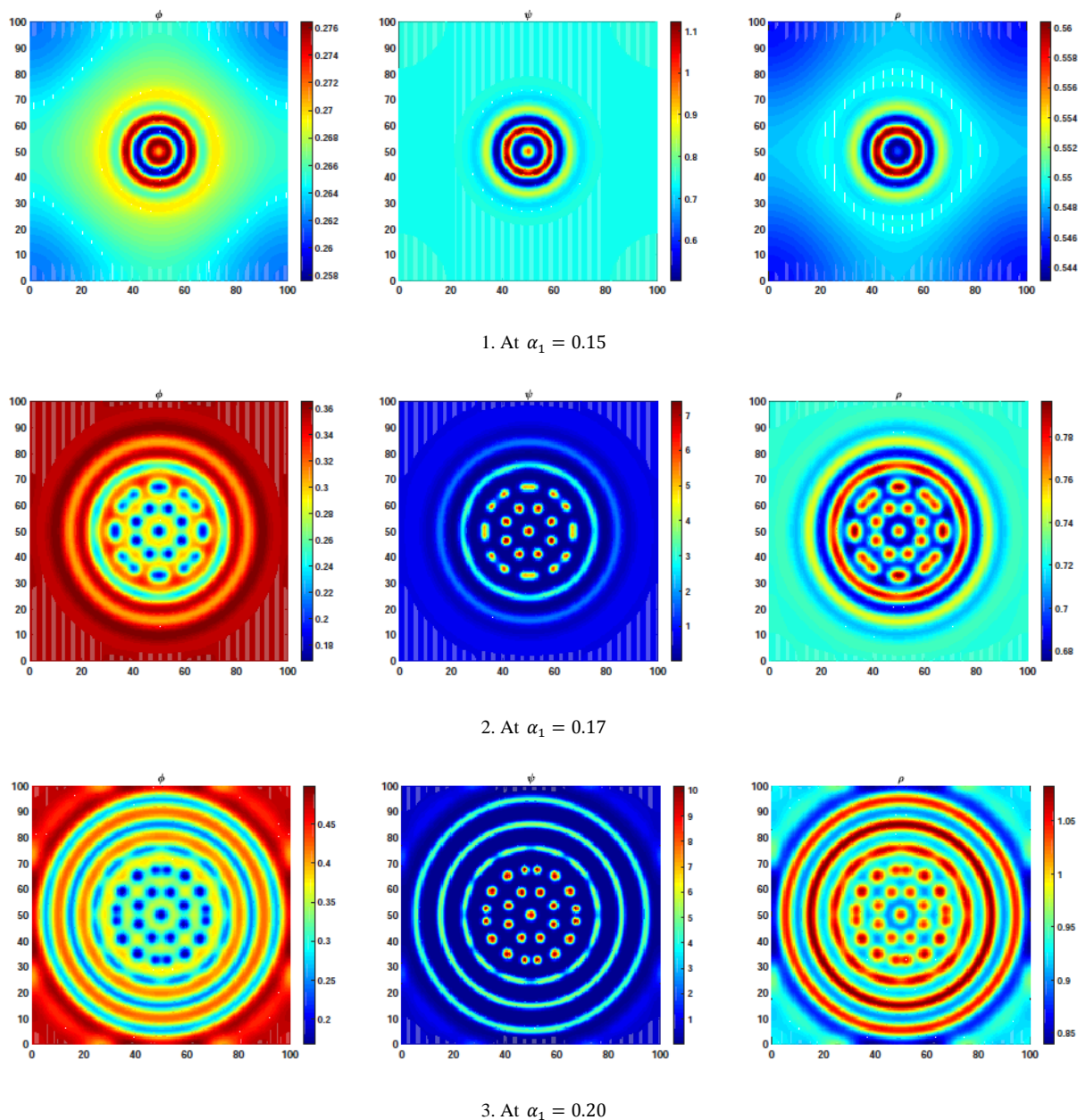


Figure 3. Snapshots of contour pictures of the species ' ϕ ', ' ψ ' and ' ρ ' at 10,000 iterations with different values of α_1 and other parameters fixed: $\beta_1 = 0.3, b_0 = 0.1, s_1 = 1.0, b_1 = 0.3, \gamma_1 = 0.017, b_2 = 0.29, s_2 = 2.0, b_3 = 0.095, \gamma_2 = 0.025, d_1 = 1.5, d_2 = 0.01$ and $d_3 = 1$

And the value of k_T^2 is given by

$$k_T^2 = \frac{-\Lambda_2 + \sqrt{(\Lambda_2^2 - 3\Lambda_1\Lambda_3)}}{3\Lambda_1} \tag{11}$$

Hence the condition of Turing instability is derived.

5. Numerical Simulations and Results

In this section, a numerical investigation is carried out for the specific set of parameters values and diffusion coefficients of the model (1) and the emergence of spatial patterns formations is discussed due to self-diffusion.

For example, we consider the following parameter values;

$$\begin{aligned}\alpha_1 &= 0.2, \beta_1 = 0.3, b_0 = 0.1, s_1 = 1.0, b_1 = 0.3, \\ \gamma_1 &= 0.017, b_2 = 0.29, \\ s_2 &= 2.0, b_3 = 0.095, \\ \gamma_2 &= 0.025,\end{aligned}\quad (12)$$

$$d_2 = 0.01 \text{ and } d_3 = 1$$

For the fixed values of parameters, we calculate the stable co-existence equilibrium point $E^* = (0.472, 0.714, 0.925)$. For numerical simulation we use finite difference method that reveals spatiotemporal complexity of the system. The simulation space size is 100×100 with time-step $\Delta t = 0.1$ and space-step ($\Delta x = 0.5 = \Delta y$). We have exhibited Turing instability and corresponding spatial patterns for the system (1). The Turing instability conditions have been obtained theoretically in Sec. (4), and whether these conditions are satisfied with the parameter values is yet to be examined. Now, we draw the graph of the Turing instability condition for different values of diffusion coefficients d_1 and other remaining parameters are fixed given in Eq. (12). Figure (1) represents the region for the orientation of spatial pattern formation corresponding to Turing-function versus the wavenumber (k).

We have represented the different types of spatial patterns formed due to the controlled parameters (d_1, α). Figure (2) exhibits the 2-D spatial pattern formation of the system (1) at 1,000, 5,000, and 10,000 iterations respectively with $d_1 = 2$ and remaining parameters are fixed as given in Eq. (12).

Figure (3) exhibits the 2-D spatial pattern formation due to control parameter ' α ' at 0.15, 0.17, 0.20 respectively. As we vary the value of the control parameters, the interesting Turing patterns are obtained such as strips, spots and mixed. In Figure's (2), (3) the blue color represents the low population density and red color represents the high population in the domain area.

6. Conclusions

We investigated the analytical study of the food web of three species with self-diffusion in this article. We obtained the uniform steady-state and derived the stability condition. We discovered the condition for Turing instability while studying the spatiotemporal model, where the system loses its stability and becomes unstable, resulting in a variety of patterns that reveal the spatial complexity of reaction-diffusion systems.

In this study, we used d_1 as the prey diffusion coefficient and α_1 as the birth rate as a controlled parameter. The patterns change and converge to stable patterns as the iteration with diffusion coefficient ($d_1=2$) increases (see Figure (2)). Variations in the prey birth rate

coefficient (α_1) result in the formation of various patterns (see Figure (3)). Ecologically, as the growth rate of prey increases, so does the population density of middle and top predators, which helps to maintain an ecological balance in the food web. The methods and results presented in this article may contribute to the study of pattern formation in the food web and explain many field observations (chemistry, epidemiology, ecology etc.).

REFERENCES

- [1] Ajraldi, V., Pittavino, M., and Venturino, E., "Modeling herd behavior in population systems," *Nonlinear Analysis: Real World Applications*, vol.12, pp. 2319–2338, 2011.
- [2] Yuan, S., Xu, C., and Zhang, T., "Spatial dynamics in a predator–prey model with herd behavior," *Chaos*, vol. 23, 033102, 2013.
- [3] Singh, T., and Banerjee, S., "Spatiotemporal model of a predator–prey system with herd behavior and quadratic mortality," *International Journal of Bifurcation and Chaos*, vol. 29, 1950049, 2019.
- [4] Ma, X., Shao, Y., Wang, Z., et al., "An impulsive two-stage predator–prey model with stage-structure and square root functional responses," *Mathematics and Computers in Simulation*, vol. 119, pp. 91–107, 2016.
- [5] Naji, R. K., and Balasim, A. T., "Dynamical behavior of a three species food chain model with Beddington-DeAngelis functional response," *Chaos, Solitons & Fractals*, vol. 32, pp. 1853–1866, 2007.
- [6] Ali, S. J., Arifin, N. M., Naji, R. K., Ismail, F., and Bachok, N., "Analysis of ecological model with holling type IV functional response," *International Journal of Pure and Applied Mathematics*, vol. 106, pp. 317–331, 2016.
- [7] Lv, S., and Zhao, M., "The dynamic complexity of a three species food chain model," *Chaos, Solitons & Fractals*, vol. 37, pp.1469–1480, 2008.
- [8] Guo, G. and Wu, J., "The effect of mutual interference between predators on a predator-prey model with diffusion," *Journal of Mathematical Analysis and Applications*, vol. 389, pp.179–194, 2012.
- [9] Turing, A. M., "The chemical basis of morphogenesis," *Philosophical Transactions of the Royal Society B*, vol. 237, pp.37–72, 1952.
- [10] Levin, S. A., and Segel, L. A., "Hypothesis for origin of planktonic patchiness," *Nature*, vol. 259, pp. 659–659, 1976.
- [11] Segel, L. A., and Jackson, J. L., "Dissipative structure: an explanation and an ecological example," *Journal of Theoretical Biology*, vol. 37, pp.545–559, 1972.
- [12] Kooi, B. W., and Venturino, E., "Ecoepidemic predator–prey model with feeding satiation, prey herd behavior and abandoned infected prey," *Mathematical Biosciences*, vol. 274, pp.58–72, 2016.

- [13] Xu, C., Yuan, S., and Zhang, T., "Global dynamics of a predator-prey model with defense mechanism for prey," *Applied Mathematics Letters*, vol. 62, pp.42-48, 2016.
- [14] Liu, X., Zhang, T., Meng, X., and Zhang, T., "Turing-Hopf bifurcations in a predator-prey model with herd behavior, quadratic mortality and prey-taxis," *Physica A: Statistical Mechanics and its Applications*, vol. 496, pp.446-460, 2018.
- [15] Tang, X., and Song, Y., "Bifurcation analysis and Turing instability in a diffusive predator-prey model with herd behavior and hyperbolic mortality," *Chaos, Solitons & Fractals*, vol. 81, pp.303-314, 2015.
- [16] Adeniji, A. A., Noufe, H. A., Mkolesia, A. C., Shatalov, M. Y., "An Approximate Solution to Predator-prey Models Using The Differential Transform Method and Multi-step Differential Transform Method, in Comparison with Results of The Classical Runge-kutta Method," *Mathematics and Statistics*, 9(5), pp.799-805, 2021. DOI: 10.13189/ms.2021.090520